Click Here for Full Article

Nuclear winter revisited with a modern climate model and current nuclear arsenals: Still catastrophic consequences

Alan Robock,[1] Luke Oman,[1,2] and Georgiy L. Stenchikov[1]

[1]   Twenty years ago, the results of climate model simulations of the response to smoke and dust from a massive nuclear exchange between the superpowers could be summarized as "nuclear winter," with rapid temperature, precipitation, and insolation drops at the surface that would threaten global agriculture for at least a year. The global nuclear arsenal has fallen by a factor of three since then, but there has been an expansion of the number of nuclear weapons states, with additional states trying to develop nuclear arsenals. We use a modern climate model to reexamine the climate response to a range of nuclear wars, producing 50 and 150 Tg of smoke, using moderate and large portions of the current global arsenal, and find that there would be significant climatic responses to all the scenarios. This is the first time that an atmosphere-ocean general circulation model has been used for such a simulation and the first time that 10-year simulations have been conducted. The response to the 150 Tg scenario can still be characterized as "nuclear winter," but both produce global catastrophic consequences. The changes are more long-lasting than previously thought, however, because the new model, National Aeronautics and Space Administration Goddard Institute for Space Studies ModelE, is able to represent the atmosphere up to 80 km, and simulates plume rise to the middle and upper stratosphere, producing a long aerosol lifetime. The indirect effects of nuclear weapons would have devastating consequences for the planet, and continued nuclear arsenal reductions will be needed before the threat of nuclear winter is removed from the Earth.

Citation: Robock, A., L. Oman, and G. L. Stenchikov (2007), Nuclear winter revisited with a modern climate model and current nuclear arsenals: Still catastrophic consequences, *J. Geophys. Res.*, *112*, D13107, doi:10.1029/2006JD008235.

1. Introduction

[2] As first suggested by *Crutzen and Birks* [1982], climate model simulations by *Turco et al.* [1983] and *Aleksandrov and Stenchikov* [1983] showed that a full-scale nuclear war would produce surface temperature, precipitation, and insolation reductions so large that the climatic consequences were described as "nuclear winter." Soon after the world was confronted with the prospect of potential indirect effects of nuclear war much larger than the direct effects, and starvation of billions of people from the collapse of world agriculture, the arms race and cold war ended. Since then, the global nuclear arsenal has been reduced by a factor of three.

[3] Prompted by the recent work of *Toon et al.* [2007] and *Robock et al.* [2007], who showed that a regional nuclear conflict using 100 Hiroshima-size (15 kt) nuclear weapons, only 0.03% of the explosive power of the current global arsenal, would produce climate change unprecedented in

human history, we revisit the nuclear winter issue with a modern climate model. We ask the question of whether the current nuclear arsenal could still produce a nuclear winter.

[4] All previous simulations of the climatic response to the smoke generated from a nuclear war were limited by computer power and the available climate models. As shown in Table 1, each simulation addressed certain aspects of the climate model response with simple climate models or with short simulations of low-resolution atmospheric general circulation models (GCMs), but now for the first time we use a coupled atmosphere-ocean GCM run continuously for multiple 10-year simulations and with a model top at the mesopause.

[5] Some critics of previous nuclear winter results suggested that once uncertainties were addressed, the severity of the results would decrease. Because of the use of the term "nuclear autumn" by *Thompson and Schneider* [1986], even though the authors made clear that the climatic consequences would be large, in policy circles the theory of nuclear winter is considered by some to have been exaggerated and disproved [e.g., *Martin*, 1988]. So we are motivated to include simulations of mechanisms not previously addressed, to see whether prior results would hold up. However, unknowns by definition are unknown, and it turns out that not only do we still get a nuclear winter using the previous baseline case, but that

[1]Department of Environmental Sciences, Rutgers University, New Brunswick, New Jersey, USA.
[2]Now at Department of Earth and Planetary Sciences, Johns Hopkins University, Baltimore, Maryland, USA.

Table 1. Comparison of Climate Models Used for Previous and Current Nuclear Winter Simulations[a]

Study	Model Type	Horizontal Resolution (Latitude × Longitude)	Vertical Levels	Seasonal Cycle?/Continuous?	Model Top	Length of Simulation (× Number of Runs)
Aleksandrov and Stenchikov [1983]	AGCM	12° × 15°	2	no	tropopause	400 days (×1)
Turco et al. [1983]	SCM	none	60	no	38 km	300 days (×10)
Robock [1984]	EBM	10° × 180°	1	yes/yes	–	4 years (×9)
Covey et al. [1984]	AGCM	4.5° × 7.5°	9	yes/no	20 km	20 days (×3)
Thompson [1985]	AGCM	4.5° × 7.5°	9	yes/no	20 km	20 days (×3)
Malone et al. [1986]	AGCM	4.5° × 7.5°	20	yes/no	32 km	40 days (×8)
Ghan et al. [1988]	AGCM	4° × 5°	2	yes/no	tropopause	30 days (×21)
Pittock et al. [1989]	AGCM	4.4° × 7.5°	9	yes/no	31 km	105 days (×2)
Ghan [1991]	AGCM	4° × 5°	2	yes/yes	tropopause	1.5 years (×3)
Current work	AOGCM	4° × 5°	23	yes/yes	80 km	10 years (×8)

[a]AGCM, atmospheric general circulation model; SCM, single column model; EBM, energy balance model; AOGCM, atmosphere-ocean general circulation model.

the climate response is much longer than that of earlier results, and current nuclear arsenals can still produce a nuclear winter.

2. Previous Nuclear Winter Simulations

[6] Before describing our work, we summarize the work done before (Table 1), and the limitations of each of these studies. *Pittock et al.* [1986], *Turco et al.* [1990], and *Sagan and Turco* [1990] summarized much of the early work, and we know of no climate modeling done on this topic in almost 20 years, other than our other recent work.

[7] *Crutzen and Birks* [1982] first suggested that the smoke from fires and dust from the surface generated by nuclear explosions from a full-scale nuclear war between the United States and the Soviet Union would be so extensive as to cause global climate change. The first climate model simulation of the response, by *Aleksandrov and Stenchikov* [1983], used a very low resolution (12° × 15° lat-lon) atmospheric GCM with only 2 levels in the vertical coupled to a mixed-layer ocean and annual average solar radiation, and conducted one 400-day simulation. Forced by the smoke estimated from a scenario using about 1/3 of the then-current arsenal, about 150 Tg, they found large surface temperature reductions, to temperatures far below freezing, and produced an overturning atmospheric circulation cell transporting the aerosols globally.

[8] *Turco et al.* [1983] used a single column model with no surface heat capacity, intended to simulate midcontinent conditions. Looking at a large number of different scenarios, they were able to model the detailed vertical evolution of climate response, but were not able to look at dynamical responses or the spatial distribution of climate change. They also gave the name "nuclear winter" to this work, capturing the forcing and response in a two-word phrase.

[9] *Covey et al.* [1984] and *Thompson* [1985] used the National Center for Atmospheric Research atmospheric GCM for short runs and looked at the seasonal cycle of climate response. Their results validated the earlier GCM results of *Aleksandrov and Stenchikov* [1983]. *Robock* [1984] used an energy-balance model with a mixed-layer ocean, and was the first to examine the seasonal cycle and interannual responses. Using the assumed short atmospheric smoke lifetime from *Turco et al.* [1983], he nevertheless found multiannual cooling prolonged by snow and sea ice feedbacks. This result was later validated with GCM simulations using a mixed-layer ocean [*Schneider and Thompson*, 1988; *Ghan*, 1991]. *Malone et al.* [1986] showed that lofting of aerosols in the summer due to solar heating would prolong their lifetime, because in the stratosphere they are removed from precipitation scavenging, but used a model with a low top of the atmosphere (32 km) and were only able to run it for 40 days.

[10] *Ghan et al.* [1988] used a simple two-layer atmospheric GCM to investigate the short-term (1 month) response to many different scenarios of different smoke properties and different model parameterizations. *Pittock et al.* [1989] investigated short-term hydrological effects for small smoke amounts with a specified optical depth of 0.2, but based this on previous results which underestimated the smoke lifetimes.

[11] *Turco et al.* [1990] showed that the original *Turco et al.* [1983] results were robust, and described how subsequent work filled in the details of the emissions of smoke, smoke properties, and climate response. Our experiment extends the time and sophistication of climate model capabilities, and shows an extended timescale of climate response not possible with previous models. However, the basic conclusion that a large-scale nuclear conflict would have devastating climatic consequences is not only supported, but strengthened.

3. Climate Model

[12] We conducted climate model simulations with a state-of-the-art general circulation model, ModelE from the National Aeronautics and Space Administration Goddard Institute for Space Studies [*Schmidt et al.*, 2006], which includes a module to calculate the transport and removal of aerosol particles [*Koch et al.*, 2006]. The atmospheric model is connected to a full ocean general circulation model with calculated sea ice, thus allowing the ocean to respond quickly at the surface and on yearly timescales in the deeper ocean. We run the atmospheric portion of the model at 4° × 5° latitude-longitude resolution, with 23 vertical layers extending to a model top of 80 km. The coupled oceanic general circulation model

Table 2. Approximate Number of Nuclear Weapons in the Arsenals of Different Countries[a]

Country	Number of Weapons
Russia	10,000
United States	10,000
France	350
China	200
Britain	200
Israel	75–200
India	40–50
Pakistan	<50
North Korea	<15

[a]From *International Panel on Fissile Materials* [2006, Table 2.1], with original data from *Norris and Kristensen* [2006]. The totals for the United States and Russia do not include warheads awaiting dismantlement.

[*Russell et al.*, 1995] has 13 layers and also a $4° \times 5°$ latitude-longitude resolution.

[13] This climate model has been tested extensively in global warming experiments [*Hansen et al.*, 2005; *Schmidt et al.*, 2006] and to examine the effects of volcanic eruptions on climate. The climate model (with a mixed-layer ocean) does an excellent job of modeling the climatic response to the 1783 Laki [*Oman et al.*, 2006b] and the 1912 Katmai [*Oman et al.*, 2005] volcanic eruptions. We have also used this model to simulate the transport and removal of sulfate aerosols from tropical and high-latitude volcanic eruptions [*Oman et al.*, 2006a], and have shown that it does a good job of simulating the lifetime and distribution of the volcanic aerosols. In the stratosphere, these aerosols have an e-folding residence time of 12 months in the model, in excellent agreement with observations.

[14] The aerosol module [*Koch et al.*, 2006] accounts for black carbon particles. We assigned an effective radius of 0.1 μm to the soot particles, a standard value based on observations. At visible wavelengths, we assign the following optical properties to the black carbon particles: mass extinction coefficient of 5.5 m^2/g, single scattering albedo of 0.64, and mass absorption coefficient of 2.0 m^2/g. These are typical of a mixture of black soot, smoke, and dust that would be injected into the atmosphere using the baseline scenario of *Turco et al.* [1983].

[15] While *Warren and Wiscombe* [1985] and *Ledley and Thompson* [1986] suggested that soot falling on sea ice would increase the albedo and negate some of the cooling from a massive atmospheric aerosol loading, *Vogelmann et al.* [1988] used the *Robock* [1984] energy-balance climate model and showed that this effect would only be important with enough solar insolation to make snow and ice albedo important. By the time the atmosphere was clear enough, *Vogelmann et al.* showed that clean snow would have fallen on the dirty snow, making the effect small. Nevertheless, we included this feedback in the runs presented here.

[16] We conducted two 10-year runs, one with 150 Tg of smoke and one with 50 Tg of smoke, injected into the upper troposphere (300–150 mbar) over a one-week period starting on 15 May spread over all the grid boxes over the 48 United States and over Russia. While *Turco et al.* [1983] used 225 Tg of smoke for their baseline case and *Covey et al.* [1984] used 200 Tg of smoke, we decided to use two scenarios that would be possible today. *Turco et al.* [1990]

give a range of 20–290 Tg of smoke injection over the Northern Hemisphere, and our 150 Tg case is just in the middle of this range. We conducted a 30-year control run with no smoke aerosols and these two 10-year simulations with smoke, starting from arbitrary initial conditions. With such a large forcing, chaotic weather variations would produce very small changes compared to the large response, so we do not produce an ensemble of runs. This was verified with a much smaller forcing of 5 Tg of aerosols in our earlier work [*Robock et al.*, 2007].

[17] The 5 Tg case [*Robock et al.*, 2007] differed from the current 50 Tg and 150 Tg cases in several ways in addition to the amount of smoke. In the 5 Tg case, all the aerosols were put into the atmosphere during a 1-day period into one model grid box at 30°N, 70°E. While also put into the 300–150 mbar layer, they were put into higher model layers for the 5 Tg case, as this layer is at a higher elevation in lower latitudes. In addition, the optical properties of the black carbon aerosols were set to those of pure smoke, as that experiment was designed to study the effects of smoke from city targets. The mass extinction coefficient was 9.0 m^2/g and the single scattering albedo was 0.31, so the mass absorption coefficient was 6.21 m^2/g. Thus per unit mass, the aerosols in the 5 Tg case would be expected to absorb more solar radiation, producing more lofting.

[18] We do not conduct detailed new studies of the smoke and dust emissions from nuclear attacks here. Rather, we chose emissions based on previous studies so as to make our results comparable to them. *Toon et al.* [2007] point out that cities around the world have grown in the past 20 years, so that we would expect smoke emissions to be larger than before for the same targets. We encourage new analyses of the exact amount of smoke that would result, but it is beyond the scope of this paper. Roughly 150 Tg would be emitted by the use of the entire current global nuclear arsenal, with 5000 Mt explosive power, about 95% of which is in the arsenals of the United States and Russia (Table 2), and 50 Tg would be emitted by the use of 1/3 of the current nuclear arsenal.

4. Results for the 150 Tg Case

[19] As found by *Robock et al.* [2007] for a 5 Tg case, the black carbon particles in the aerosol layer for the 150 Tg case are heated by absorption of shortwave radiation and lofted into the upper stratosphere. The aerosols quickly spread globally and produce a long-lasting climate forcing (Figure 1). They end up much higher than is typical of weakly absorbing volcanic sulfate aerosols, which typically are just above the tropopause [*Stenchikov et al.*, 1998]. As a result, the soot aerosols have a very long residence time and continue to affect surface climate for more than a decade. The mass e-folding time for the smoke is 4.6 years, as compared to 1 year for typical volcanic eruptions [*Oman et al.*, 2006a] and 1 week for tropospheric aerosols. After 4.6 years, the e-folding time is reduced, but is still longer than that of volcanic aerosols. In addition to the lofting of the smoke by solar absorption, another reason for this difference is that volcanic sulfate aerosols are larger, with an effective radius of 0.5 μm, and thus they have a higher settling velocity than the smaller smoke aerosols. This long smoke aerosol lifetime is different from results found in
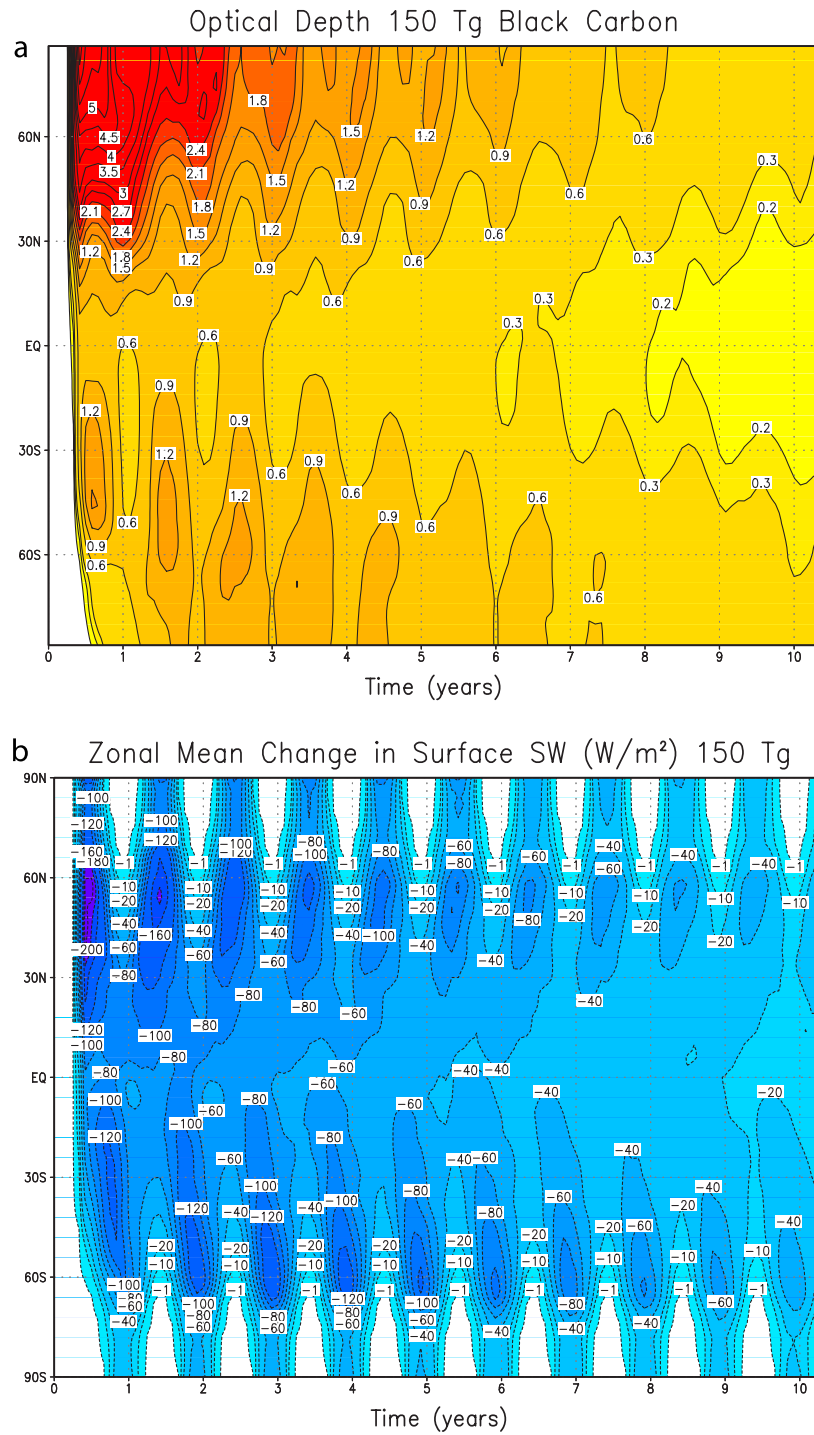
Figure 1. Changes in visible optical depth and net downward shortwave radiation at the surface for the 150 Tg case. Although the maximum forcing is in the Northern Hemisphere during the first summer, the aerosols rapidly spread around the globe producing large solar radiation reductions in both hemispheres.

previous nuclear winter simulations, which either fixed the vertical extent of the aerosols [*Turco et al.*, 1983] or used older-generation climate models with limited vertical resolution and low model tops [*Aleksandrov and Stenchikov*, 1983; *Covey et al.*, 1984; *Malone et al.*, 1986], artificially limiting the particle lifetimes.

[20] The maximum change in net global average surface shortwave radiation for the 150 Tg case is -100 W m^{-2} (Figure 2). This negative forcing persists for many years, with the global average value still at -20 W m^{-2} even 10 years after the initial smoke injection. This forcing greatly exceeds the maximum global average surface forc-
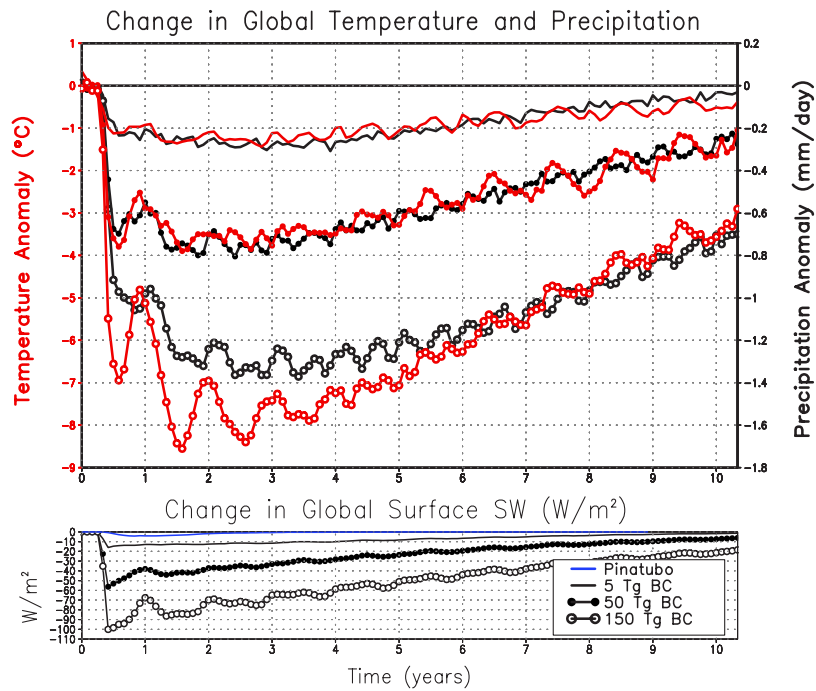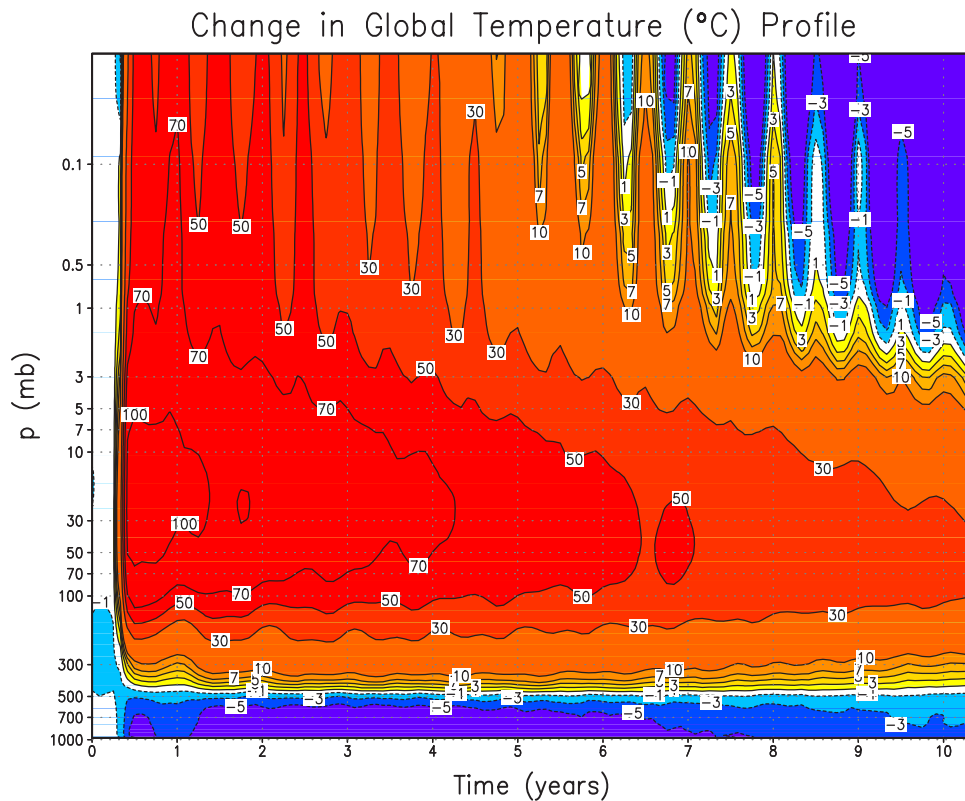
Figure 2. Change of global average surface air temperature, precipitation, and net downward shortwave radiation for the 5 Tg [*Robock et al.*, 2007], 50 Tg and 150 Tg cases. Also shown for comparison is the global average change in downward shortwave radiation for the 1991 Mt. Pinatubo volcanic eruption [*Oman et al.*, 2005], the largest volcanic eruption of the 20th century. The global average precipitation in the control case is 3.0 mm/day, so the changes in years 2−4 for the 150 Tg case represent a 45% global average reduction in precipitation.
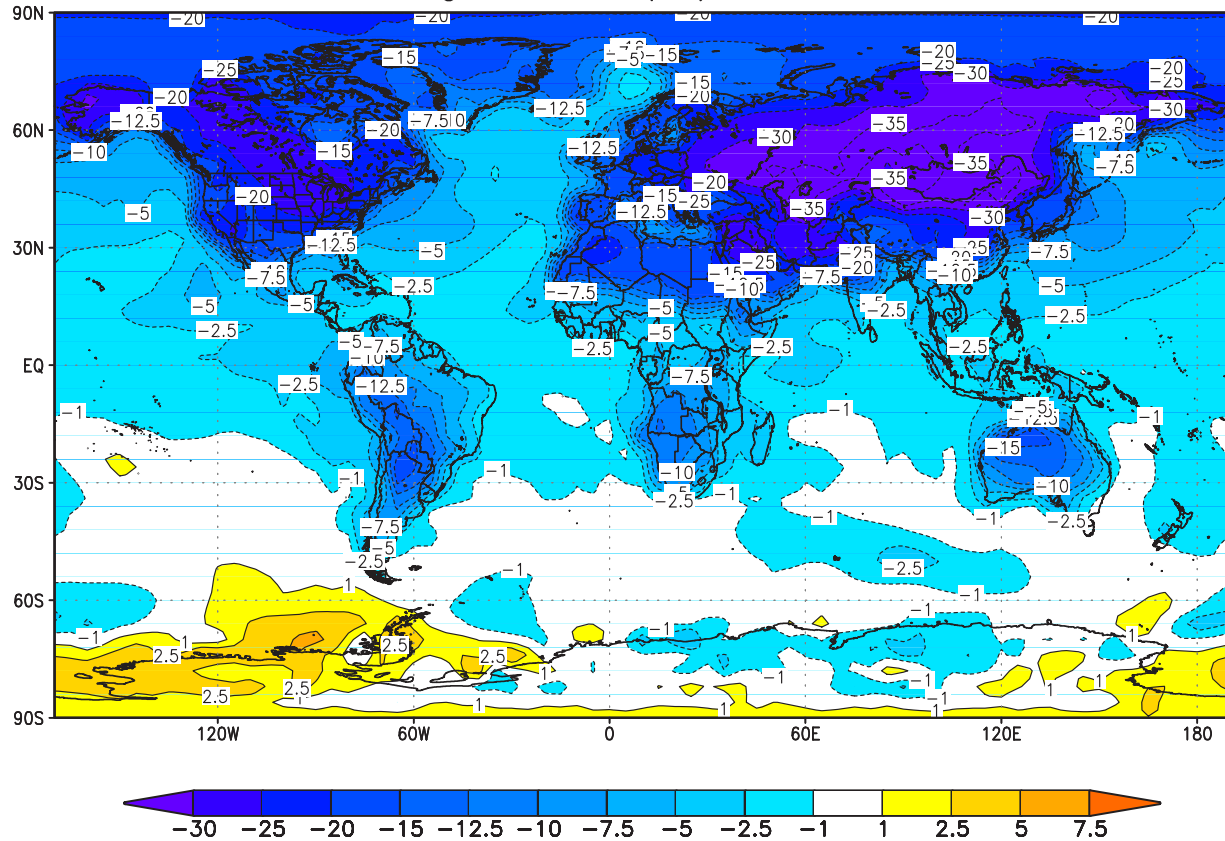

Figure 3. Change in global average temperature (°C) profile for the 150 Tg case from the surface to 0.02 mbar [80 km]. The semiannual periodicity at the top is due to enhanced heating during the summers in each hemisphere.

Figure 4. Surface air temperature changes for the 150 Tg case averaged for June, July, and August of the year of smoke injection and the next year. Effects are largest over land, but there is substantial cooling over oceans, too. The warming over Antarctica in year 0 is for a small area, is part of normal winter interannual variability, and is not significant. Also shown as red circles are two locations in Iowa and Ukraine, for which time series of temperature and precipitation are shown in Figures 5 and 7.

ing of -4 W m^{-2} for the 1991 Mt. Pinatubo volcanic eruption [*Kirchner et al.*, 1999; *Oman et al.*, 2005], the largest of the 20th century, also shown in Figure 2. The volcanic forcing disappeared with an e-folding time of only 1 year, and during the first year averaged -3.5 W m^{-2} (Figure 2).

[21] The effects of the smoke cloud on surface temperature are extremely large (Figure 2). Stratospheric temperatures are also severely perturbed (Figure 3). A global average surface cooling of $-7°C$ to $-8°C$ persists for years, and after a decade the cooling is still $-4°C$ (Figure 2). Considering that the global average cooling at the depth of the last ice age 18,000 years ago was about $-5°C$, this would be a climate change unprecedented in speed and amplitude in the history of the human race. The temperature changes are largest over land. Maps of the temperature changes for the Northern Hemisphere summers for the year of smoke injection (year 0) and the next year (year 1) are shown in Figure 4. Cooling of more than $-20°C$ occurs over large areas of North America and of more than $-30°C$ over much of Eurasia, including all agricultural regions. There are also large temperature changes in the tropics and over Southern Hemisphere continents. Large climatic

effects would occur in regions far removed from the target areas or the countries involved in the conflict.

[22] As examples of the actual temperature changes in important grain-growing regions, we have plotted the time series of daily minimum air temperature for grid points in Iowa, United States, at 42°N, 95°W, and in Ukraine at 50°N, 30°E (Figure 5). For both locations (shown in Figure 4), minimum temperatures rapidly plummet below freezing and stay there for more than a year. In Ukraine, they stay below freezing for more than two years. Clearly, this would have agricultural implications.

[23] As a result of the cooling of the Earth's surface, evapotranspiration is reduced and the global hydrological cycle is weakened. In addition, Northern Hemisphere summer monsoon circulations collapse, because the driving continent-ocean temperature gradient does not develop. The resulting global precipitation is reduced by about 45% (Figure 2). As an example, Figure 6 shows a map of precipitation change for the Northern Hemisphere summer one year after the smoke injection. The largest precipitation reductions are in the Intertropical Convergence Zone and in areas affected by the North American, Asian, and African summer monsoons. The small areas of increased precipita-
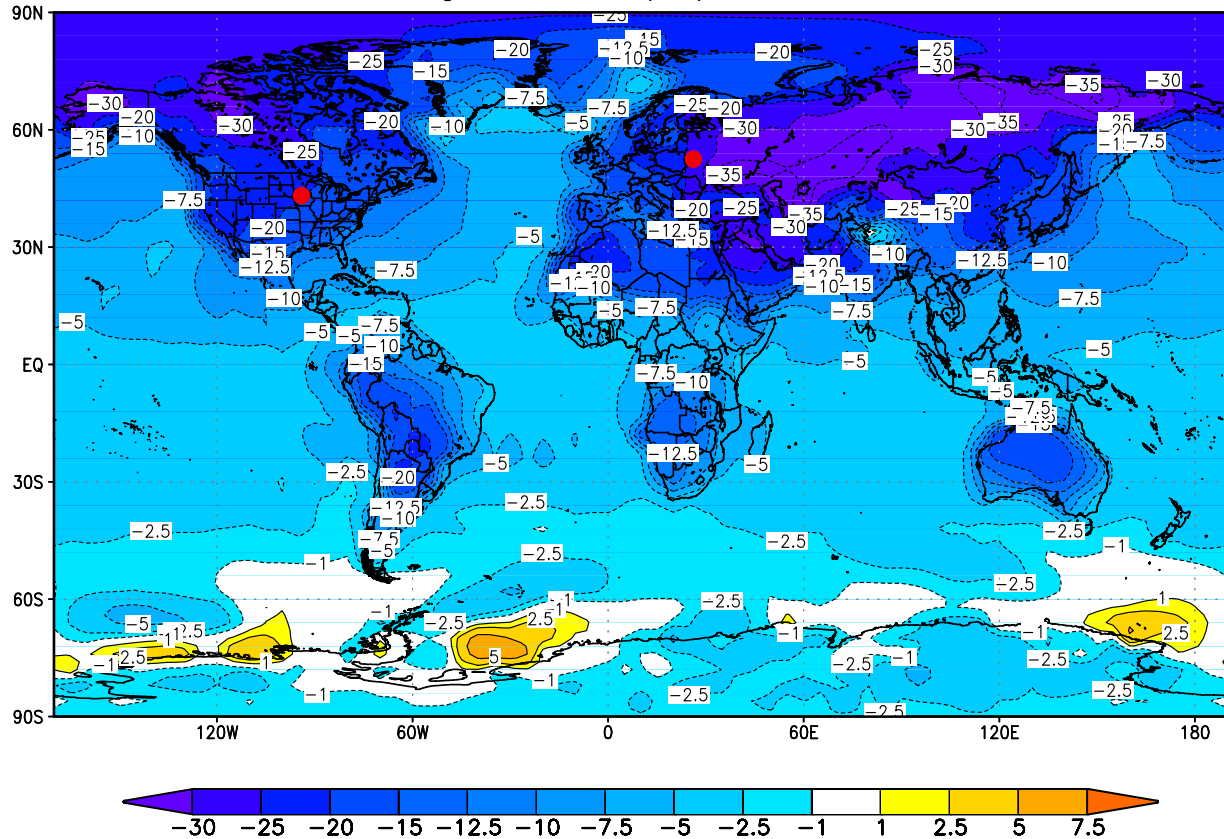
Figure 4. (continued)

tion are in the subtropics in response to a severely weakened Hadley Cell. Figure 7 shows time series of monthly precipitation for the same Iowa location as shown in Figure 5, and it is clear that these large precipitation reductions would also have agricultural implications.

[24] This is the first time an atmosphere-ocean general circulation model of the climate system has been used to study nuclear winter. It is the first one to be able to estimate the amplitude and timescale of ocean cooling, and to evaluate the time the system will need to return to the previous equilibrium. This is because the model explicitly models the effects of the thermal inertia of the ocean at different depths, as well as oceanic circulation changes. The long-lasting climate response to this smoke injection is a combination of the ability of the model to loft the soot aerosols high into the stratosphere, and of the ability of the model to calculate the characteristic response time of the climate system.

5. Results for the 50 Tg Case

[25] The 50 Tg case produced climate responses very similar to those for the 150 Tg case, but with about half the amplitude. As shown in Figure 2, the surface shortwave forcing is about half that of the 150 Tg case, and reductions of temperature and precipitation were also about half those of the 150 Tg case. However, the timescale of response is about the same. This is because in this case, too, the smoke aerosols are lofted high into the stratosphere, and have almost exactly the same stratospheric residence time, with an e-folding decay time of 5.5 years, as compared to 4.6 years for the 150 Tg case and 1 year for a typical volcanic eruption like Pinatubo. The e-folding time is about 6 years for the 5 Tg case [*Robock et al.*, 2007], even longer. The reason is that for the lower soot amounts, solar radiation can affect a larger portion of the soot and it is lofted higher. In the 150 Tg case, the large soot amounts shade some of the lower soot, and the average lofting is less, producing slightly shorter average lifetimes. For the 5 Tg case, the optical properties and more equatorward location of the initial smoke injection produce more relative solar absorption. In the case of volcanic aerosols, there is little lofting, because of the much higher albedo of the aerosols, and therefore a much shorter lifetime.

[26] The forcing and response to an input of 50 Tg are half that of the 150 Tg case even though the aerosol loading is one third, because of a saturation effect. Once almost all the solar radiation is already blocked, additional smoke aerosol particles in the larger case have less of an effect than those put into a clean atmosphere. While the maximum global average precipitation reductions for the 50 Tg case are almost exactly half of those from the 150 Tg case, the 50 Tg temperature changes less than half of those from the 150 Tg case. This difference in the nonlinearity of the response
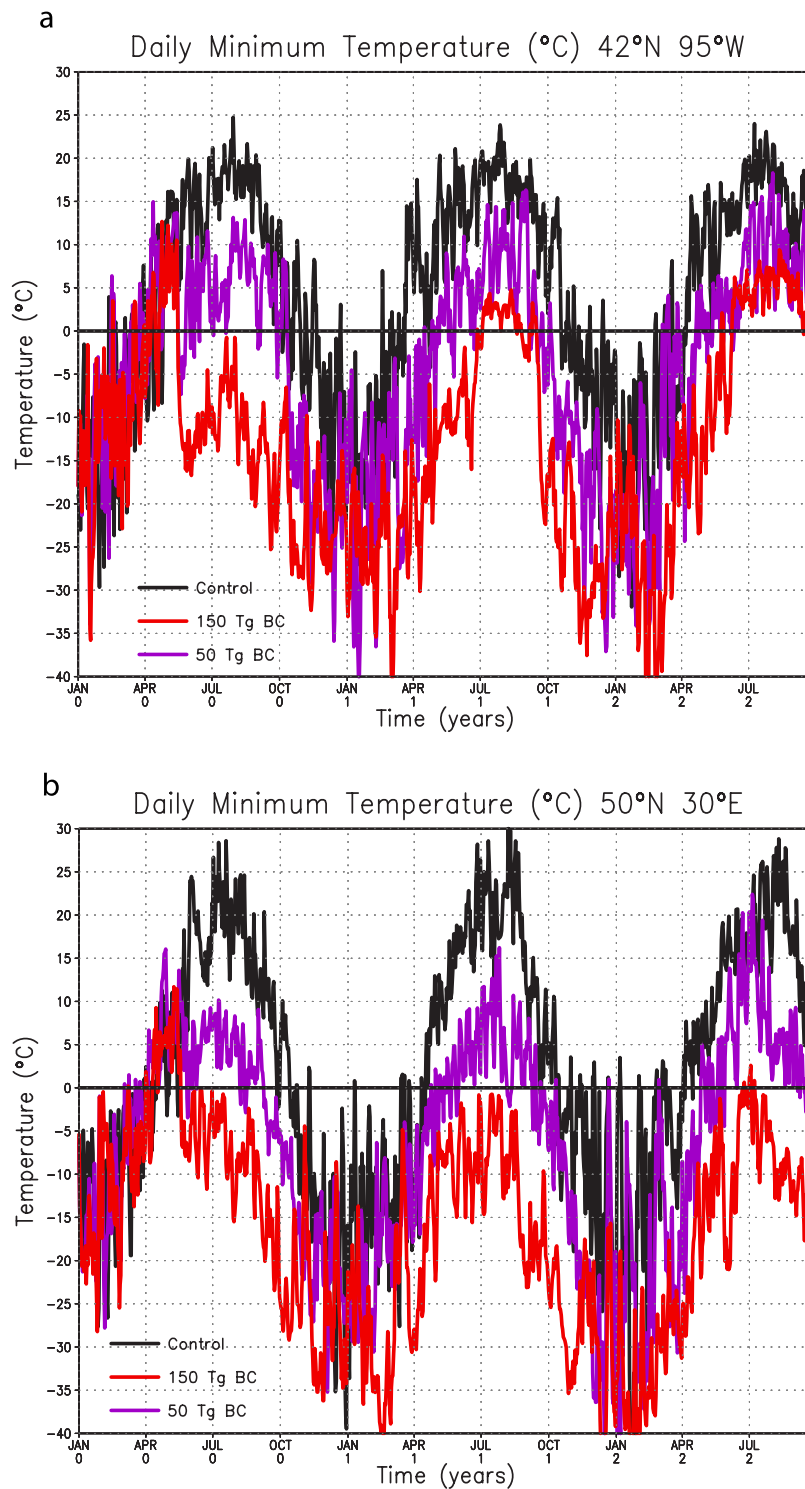
Figure 5. Time series of daily minimum temperature from the control, 50 Tg, and 150 Tg cases for two important agricultural regions, (top) Iowa, United States, at 42°N, 95°W, and (bottom) Ukraine at 50°N, 30°E. These two locations are shown on the map in Figure 4.

between temperature and precipitation is because the additional cooling in the 150 Tg case does not produce as much change in evapotranspiration, because of the exponential nature of the Clausius-Clapeyron relationship.

[27] Figures 5 and 7 also show temperature and precipitation time series for the 50 Tg case for the Iowa and Ukraine locations. The effects here are approximately half those of the 150 Tg case. While these temperature responses

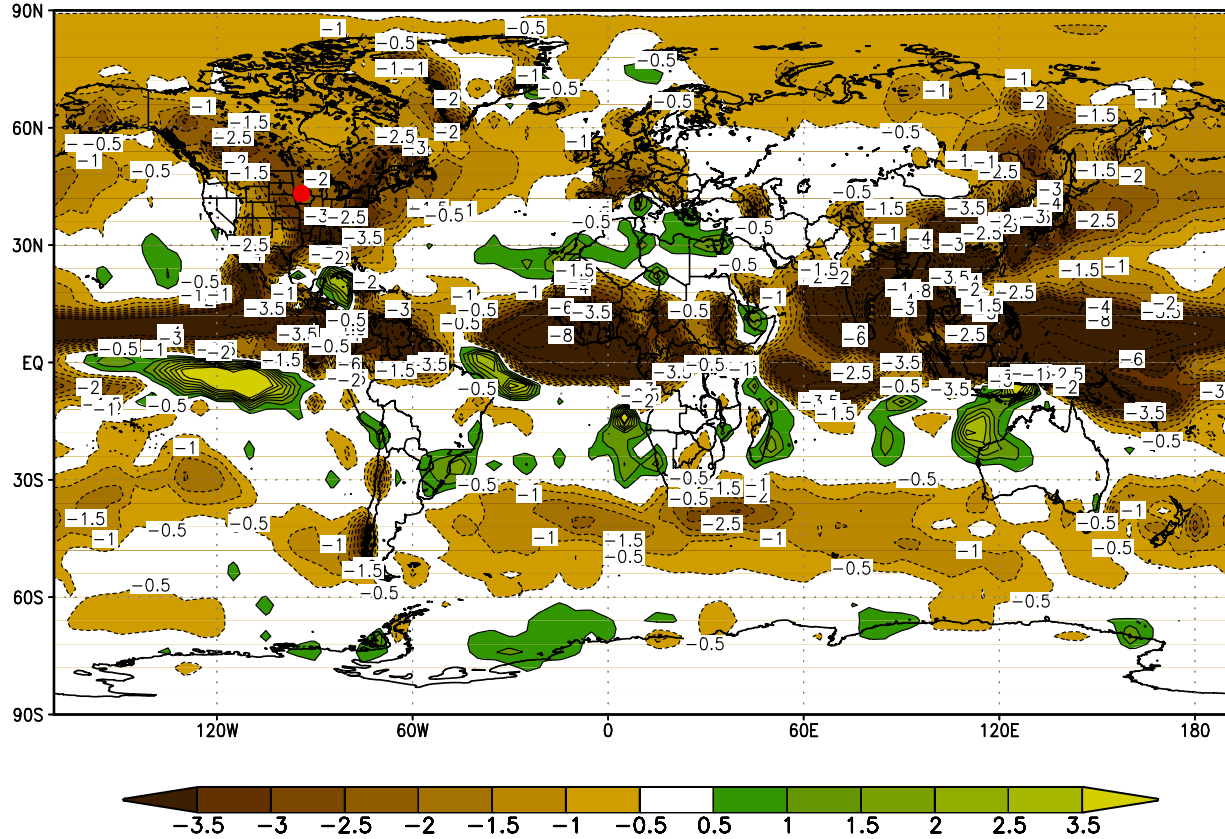## Change in Precipitation (mm/day) JJA Year 1

Figure 6. Precipitation changes (mm/day) in response to the 150 Tg case averaged for June, July, and August of the first year following the smoke injection. There are large reductions over large regions, especially those affected by the North American, Asian, and African summer monsoons. The small areas of increased precipitation are in the subtropics in response to a severely weakened Hadley Cell. Also shown as a red circle is the location in Iowa for which time series of precipitation are shown in Figure 7.

are not cold enough to be classified as nuclear "winter," they would still be severe and unprecedented.

6. Impacts

[28] The amplitude of the climate changes from the 5 Tg, 50 Tg and 150 Tg cases are compared to those from global warming of the past century in Figure 8 and climate change of the past 1000 years in Figure 9. In both cases it is clear that all cases would produce unprecedented long-lasting climate change. The 50 Tg and 150 Tg cases produce cooling as large or larger than that experienced 18,000 years ago during the coldest period of the last Ice Age.

[29] *Harwell and Hutchinson* [1986] clearly described the impacts of nuclear winter. They assumed that there would be no food production around the world for one year and concluded that most of the people on the planet would run out of food and starve to death by then. Our results show that this period of no food production needs to be extended by many years, making the impacts of nuclear winter even worse than previously thought.

[30] Agriculture would be affected by many factors, including temperature changes, precipitation changes, and
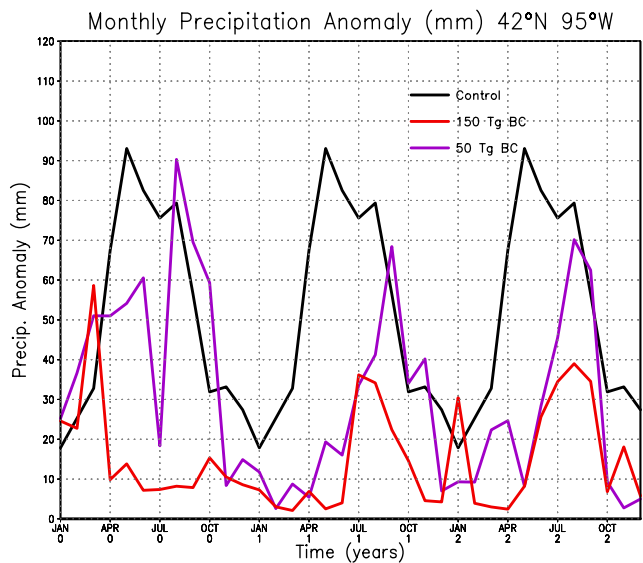

Figure 7. Time series of monthly precipitation from the control, 50 Tg, and 150 Tg cases for the important agricultural region of Iowa, United States, at 42°N, 95°W. The location is shown on the map in Figure 6.

GISS Global Average Temperature Anomaly
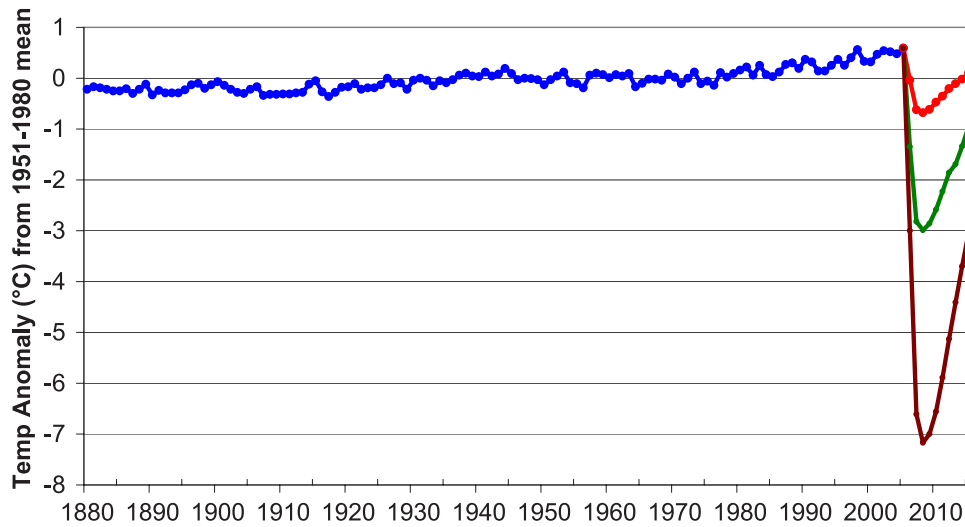**+ 5 Tg, 50 Tg, 150 Tg smoke in 2006**

Figure 8. Global average surface air temperature change from the 5 Tg (red), 50 Tg (green), and 150 Tg (brown) cases in the context of the climate change of the past 125 years. Observations are from the National Aeronautics and Space Administration Goddard Institute for Space Studies analysis [*Hansen et al.*, 2001, updated at http://data.giss.nasa.gov/gistemp/2005/].

changes in insolation [e.g., *Robock et al.*, 1993; *Maytín et al.*, 1995]. As an example, Figure 10 shows changes in the length of the freeze-free growing season for the third full growing seasons in the Northern and Southern Hemispheres. Such large reductions in growing season would completely eliminate crops that have insufficient time to reach maturity. Also, global ozone loss is likely [*Toon et al.*, 2007], with effects on downward ultraviolet radiation [*Vogelmann et al.*, 1992] and atmospheric circulation.

Mann et al. Hockey Stick, CRU Instrumental NH Temperature Anomaly
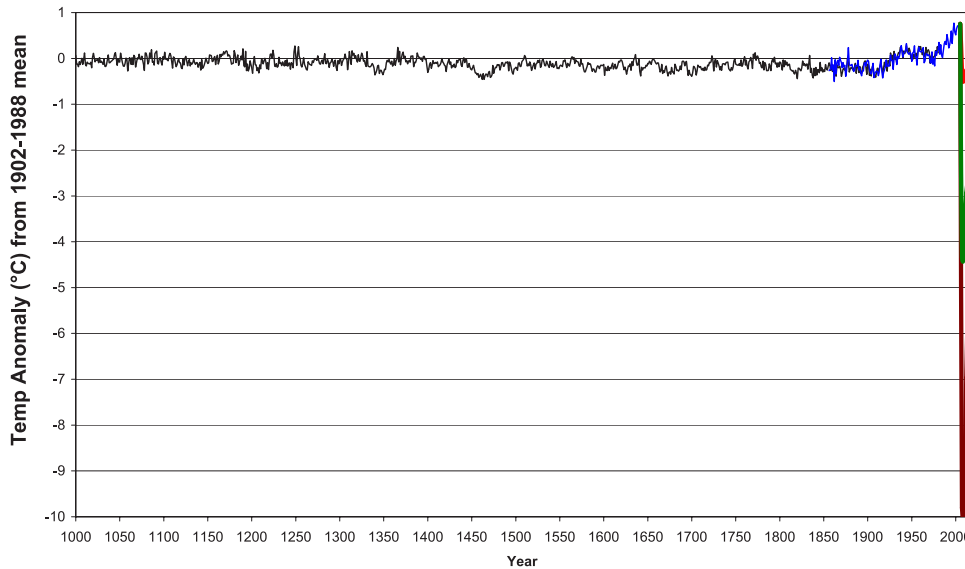**+ 5 Tg, 50 Tg, 150 Tg smoke in 2006**

Figure 9. Northern Hemisphere average surface air temperature change from 5 Tg (red), 50 Tg (green), and 150 Tg (brown) cases in the context of the climate change of the past 1000 years. The "hockey stick" nature of the curve is barely discernible when plotted on this scale. Black curve is from *Mann et al.* [1999], and the blue curve is from the latest data from the Climatic Research Unit website (http://www.cru.uea.ac.uk/cru/data/temperature/).
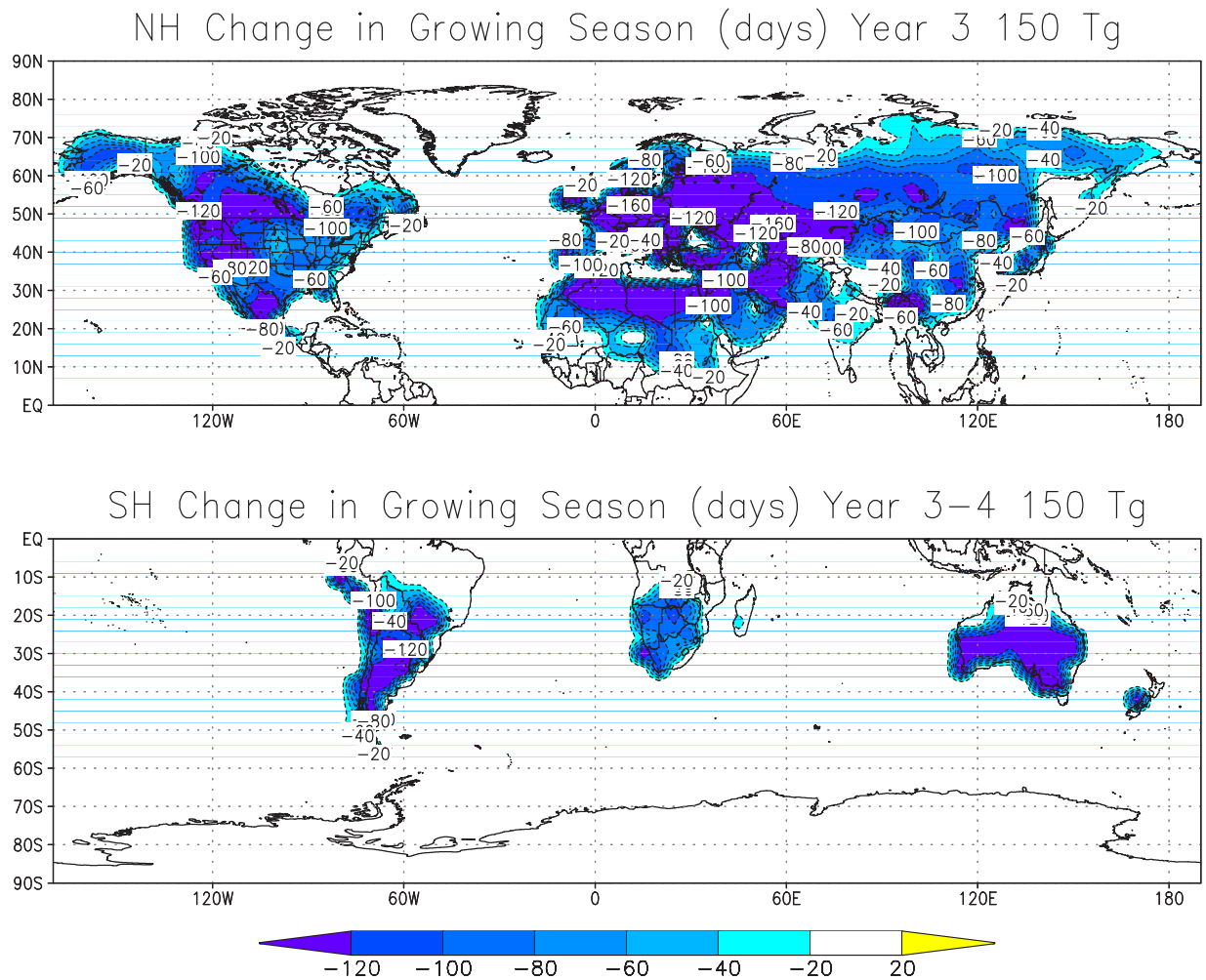
Figure 10. Change in growing season (period with freeze-free days) in the third year following the smoke injection for the 150 Tg and 50 Tg cases.

Further analysis of these and other effects, which is beyond the scope of this paper, is needed.

7. Uncertainties

[31] The calculations presented here, combined with the 5 Tg case of *Robock et al.* [2007], are the first ever of the effects of black carbon from nuclear conflicts with a coupled atmosphere-ocean general circulation model, presumably the most complete and accurate representation of our understanding of the climate system. Nevertheless, as pointed out by *Robock et al.* [2007], the results depend on the fidelity of the climate model we used and on the assumptions we made. The climate model has been extensively evaluated by our own volcanic cloud simulations [*Oman et al.*, 2005, 2006a, 2006b] and in international intercomparisons as part of the Fourth Assessment of the Intergovernmental Panel on Climate Change [e.g., *Miller et al.*, 2006; *Stenchikov et al.*, 2006a]. This model has a climate sensitivity in the middle of the range of other models and performs at a level equal to other state-of-the-art models. However, the experiments should be repeated with other climate models to examine how dependent the results are on the model used.

[32] We used the values of optical properties for black carbon based on those assumed in earlier nuclear winter simulations. The sensitivity of the results to these assumptions should be tested with additional experiments. We assumed that the resulting material would be initially emplaced in the upper troposphere. Although most previous simulations used a more uniform vertical distribution in the troposphere [*Turco et al.*, 1990], our assumption may be conservative as observations show direct stratospheric injections of smoke from intense Canadian and Australian forest fires [*Fromm and Servranckx*, 2003; *Jost et al.*, 2004; *Fromm et al.*, 2005, 2006]. The burning characteristics of forest fires may not be a perfect analog for cities, but firestorms with injection of smoke into the upper atmosphere were observed in previous cases of burning cities, after the earthquake-induced fire in San Francisco in 1906 [*London*, 1906] and the firebombing of Dresden in 1945 [*Vonnegut*, 1969].

[33] The relatively coarse horizontal resolution used in our atmospheric model ($4° \times 5°$ latitude-longitude) may not be adequate to simulate stratospheric lofting of the aerosols, as actual atmospheric convection occurs on smaller spatial scales. However, *Stenchikov et al.* [2006b] conducted detailed, high-resolution smoke plume simulations with the
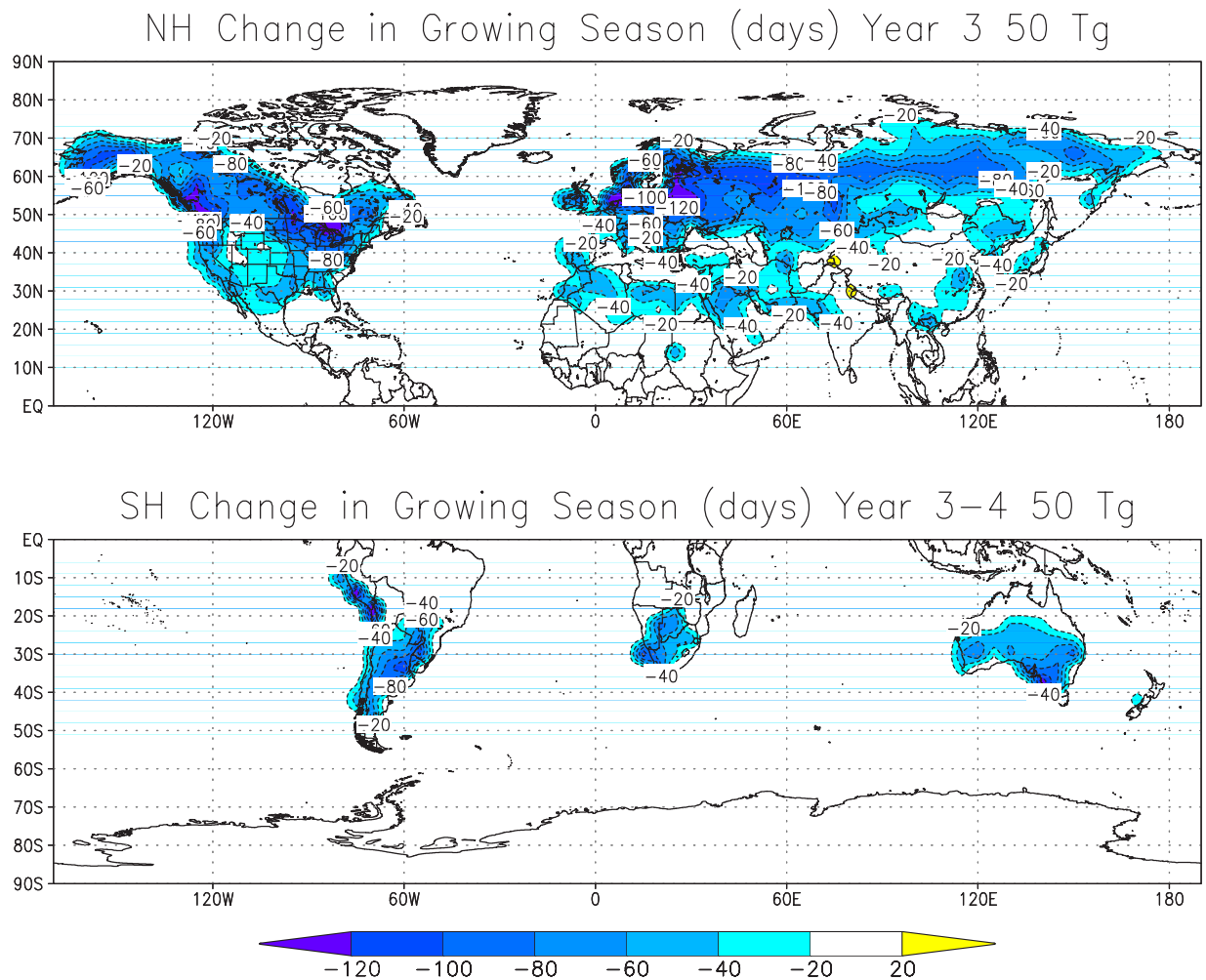
Figure 10.   (continued)

RAMS regional climate model [e.g., *Miguez-Macho et al.*, 2005] and showed that individual plumes, such as those from the Kuwait oil fires in 1991, would not be expected to loft into the upper atmosphere or stratosphere, because they become diluted. However, much larger plumes, such as would be generated by city fires, produce large, undiluted mass motion that results in smoke lofting. New large eddy simulation model results at much higher resolution also give similar lofting to our results, and no small-scale response that would inhibit the lofting [*Jensen*, 2006].

[34]   Our model does not account for coagulation of the black carbon particles, and subsequent reduction in their effects on radiation and their lifetime. However, soot aerosols tend to coagulate to chain-shaped and fluffy particles with fall velocities that are low relative to equal mass spheres. The optical properties of nonspherical carbon particles do not change significantly with particle size, as do those of spherical particles [*Nelson*, 1989]. We conducted one experiment of the 150 Tg case with 0.3 μm effective radius for the soot aerosols, and found that the e-folding lifetime was about 15% less than with 0.1 μm, 4.0 years instead of 4.6 years. So coagulation would have a small effect on the lifetime of the results here, and future experiments will include calculation of coagulation based on

aerosol concentration. Our results do not account for possible reduction in smoke absorption due to photochemical processing in the stratosphere [*Toon et al.*, 2007], which may reduce the overall lifetime of the soot.

[35]   The greatest uncertainty is the total amount of smoke. Our assumptions about smoke mass, mass absorption coefficient, and initial smoke vertical distribution all affect the amplitude of climate response, but, interestingly, not the timescale of the response. Assuming less smoke absorption or a lower smoke emplacement would make the 150 Tg results more like those of the 50 Tg case. Conversely, assuming more smoke absorption or higher emplacement would make the 50 Tg results more like the 150 Tg case.

8.   Policy Implications

[36]   The major policy implication of nuclear winter was that a full-scale nuclear attack would produce climatic effects which would so disrupt the food supply that it would be suicide for the attacking country [*Robock*, 1989] and would also impact noncombatant countries. The subsequent end of the arms race and reduction of superpower tensions can be traced back to the world being forced to confront

both the direct and indirect consequences of the use of nuclear weapons by the public policy debate in response to nuclear winter theory, but the relative impact of nuclear winter theory as compared to other factors has not been studied, as far as we know. However, the arms race ended several years before the Soviet Union collapsed. While significant reductions of American and Russian nuclear arsenals followed, our results show that each country still retains enough weapons to produce a large, long-lasting, unprecedented global climate change.

[37] "Star Wars" (Strategic Defense Initiative, now the Missile Defense Agency) is not the answer, since it still does not work after 20 years of trying. Even if it worked according to specifications, it would let in too many weapons, such as on cruise missiles. Indirect effects of nuclear winter are greater that direct effects. There would be many innocent victims in noncombatant nations.

[38] The United States and Russia are signatories to the Strategic Offensive Reductions Treaty, which commits both to a reduction to 1700–2200 deployed nuclear weapons by the end of 2012. This continuing reduction of nuclear weapons by both parties is to be commended, but only nuclear disarmament will completely remove the possibility of a nuclear environmental catastrophe. In the meantime, it is instructive to ask why Britain, France, and China have chosen nuclear arsenals of only a couple hundred nuclear weapons (Table 2). The threat of how many nuclear weapons dropping on your major cities would be necessary to deter an attack on another nuclear power? More than one? An immediate reduction of the Russian and American nuclear arsenals to the same size as those of Britain, France, and China would set an example for the world, maintain the nuclear deterrence of each, and dramatically lower the chances of nuclear winter.

[39] The results in this paper need to be tested with other climate models, and the detailed consequences on agriculture, water supply, global trade, communications, travel, air pollution, and many more potential human impacts need further study. Each of these potential hazards deserves careful scientific analysis by governments around the world.

References

Aleksandrov, V. V., and G. L. Stenchikov (1983), On the modeling of the climatic consequences of the nuclear war, *Proc. Appl. Math*, 21 pp., Comput. Cent., Russ. Acad. of Sci., Moscow.

Covey, C., S. Thompson, and S. H. Schneider (1984), Global atmospheric effects of massive smoke injections from a nuclear war: Results from general circulation model simulations, *Nature*, *308*, 21–25.

Crutzen, P. J., and J. W. Birks (1982), The atmosphere after a nuclear war: Twilight at noon, *Ambio*, *11*, 114–125.

Fromm, M. D., and R. Servranckx (2003), Transport of forest fire smoke above the tropopause by supercell convection, *Geophys. Res. Lett.*, *30*(10), 1542, doi:10.1029/2002GL016820.

Fromm, M., R. Bevilacqua, R. Servranckx, J. Rosen, J. P. Thayer, J. Herman, and D. Larko (2005), Pyro-cumulonimbus injection of smoke to the stratosphere: Observations and impact of a super blowup in northwestern Canada on 3–4 August 1998, *J. Geophys. Res.*, *110*, D08205, doi:10.1029/2004JD005350.

Fromm, M., A. Tupper, D. Rosenfeld, R. Servranckx, and R. McRae (2006), Violent pyro-convective storm devastates Australia's capital and pollutes the stratosphere, *Geophys. Res. Lett.*, *33*, L05815, doi:10.1029/2005GL025161.

Ghan, S. J. (1991), Chronic climatic effects of nuclear war, *Atmos. Environ., Part A*, *25*, 2615–2625.

Ghan, S. J., M. C. MacCracken, and J. J. Walton (1988), Climatic response to large atmospheric smoke injections: Sensitivity studies with a tropospheric general circulation model, *J. Geophys. Res.*, *93*, 8315–8337.

Hansen, J. E., R. Ruedy, M. Sato, M. Imhoff, W. Lawrence, D. Easterling, T. Peterson, and T. Karl (2001), A closer look at United States and global surface temperature change, *J. Geophys. Res.*, *106*, 23,947–23,963.

Hansen, J., et al. (2005), Efficacy of climate forcings, *J. Geophys. Res.*, *110*, D18104, doi:10.1029/2005JD005776.

Harwell, M. A., and T. C. Hutchinson (Eds.) (1986), *Environmental Consequences of Nuclear War, SCOPE 28*, vol. II, *Ecological and Agricultural Effects*, John Wiley, New York.

International Panel on Fissile Materials (2006), *Global Fissile Material Report 2006*, 99 pp., Program on Sci. and Global Security, Princeton Univ., Princeton, N.J.

Jensen, E. J. (2006), Lofting of smoke plumes generated by regional nuclear conflicts, *Eos Trans. AGU*, *87*(52), Fall Meet. Suppl., Abstract U14A-06.

Jost, H. J., et al. (2004), In-situ observations of mid-latitude forest fire plumes deep in the stratosphere, *Geophys. Res. Lett.*, *31*, L11101, doi:10.1029/2003GL019253.

Kirchner, I., G. L. Stenchikov, H.-F. Graf, A. Robock, and J. C. Antuña (1999), Climate model simulation of winter warming and summer cooling following the 1991 Mount Pinatubo volcanic eruption, *J. Geophys. Res.*, *104*, 19,039–19,055.

Koch, D., G. A. Schmidt, and C. V. Field (2006), Sulfur, sea salt, and radionuclide aerosols in GISS ModelE, *J. Geophys. Res.*, *111*, D06206, doi:10.1029/2004JD005550.

Ledley, T. S., and S. L. Thompson (1986), Potential effect of nuclear war smokefall on sea ice, *Clim. Change*, *8*, 155–171.

London, J. (1906), The story of an eyewitness, *Collier's, the National Weekly*, 5 May.

Malone, R. C., L. H. Auer, G. A. Glatzmaier, M. C. Wood, and O. B. Toon (1986), Nuclear winter: Three-dimensional simulations including interactive transport, scavenging, and solar heating of smoke, *J. Geophys. Res.*, *91*, 1039–1054.

Mann, M. E., R. S. Bradley, and M. K. Hughes (1999), Northern Hemisphere temperatures during the past millennium: Inferences, uncertainties, and limitations, *Geophys. Res. Lett.*, *26*, 759–762.

Martin, B. (1988), Nuclear winter: science and politics, *Sci. Public Policy*, *15*(5), 321–334.

Maytín, C. E., M. Acevedo, R. Jaimez, R. Andressen, M. A. Harwell, A. Robock, and A. Azócar (1995), Potential effects of global climatic change on the phenology and yield of maize in Venezuela, *Clim. Change*, *29*, 189–211.

Miguez-Macho, G., G. L. Stenchikov, and A. Robock (2005), Regional climate simulations over North America: Interaction of local processes with improved large-scale flow, *J. Clim.*, *18*, 1227–1246.

Miller, R. L., G. A. Schmidt, and D. Shindell (2006), Forced annular variations in the 20th century IPCC AR4 models, *J. Geophys. Res.*, *111*, D18101, doi:10.1029/2005JD006323.

Nelson, J. (1989), Fractality of sooty smoke: Implications for the severity of nuclear winter, *Nature*, *339*, 611–613.

Norris, R. S., and H. M. Kristensen (2006), Global nuclear stockpiles, 1945–2006, *Bull At. Sci.*, *62*(4), 64–66.

Oman, L., A. Robock, G. Stenchikov, G. A. Schmidt, and R. Ruedy (2005), Climatic response to high latitude volcanic eruptions, *J. Geophys. Res.*, *110*, D13103, doi:10.1029/2004JD005487.

Oman, L., A. Robock, G. L. Stenchikov, T. Thordarson, D. Koch, D. T. Shindell, and C. Gao (2006a), Modeling the distribution of the volcanic aerosol cloud from the 1783–1784 Laki eruption, *J. Geophys. Res.*, *111*, D12209, doi:10.1029/2005JD006899.

Oman, L., A. Robock, G. L. Stenchikov, and T. Thordarson (2006b), High-latitude eruptions cast shadow over the African monsoon and the flow of the Nile, *Geophys. Res. Lett.*, *33*, L18711, doi:10.1029/2006GL027665.

Pittock, A. B., T. P. Ackerman, P. J. Crutzen, M. C. MacCracken, C. S. Shapiro, and R. P. Turco (Eds.) (1986), *Environmental Consequences of Nuclear War, SCOPE 28*, vol. I, *Physical and Atmospheric Effects*, John Wiley, New York.

Pittock, A. B., K. Walsh, and J. S. Frederiksen (1989), General circulation model simulation of mild nuclear winter effects, *Clim. Dyn.*, *3*, 191–206.

Robock, A. (1984), Snow and ice feedbacks prolong effects of nuclear winter, *Nature*, *310*, 667–670.

Robock, A. (1989), Policy implications of nuclear winter and ideas for solutions, *Ambio*, *18*, 360–366.

Robock, A., et al. (1993), Use of general circulation model output in the creation of climate change scenarios for impact analysis, *Clim. Change*, *23*, 293–335.

Robock, A., L. Oman, G. L. Stenchikov, O. B. Toon, C. Bardeen, and R. P. Turco (2007), Climatic consequences of regional nuclear conflicts, *Atmos. Chem. Phys.*, *7*, 2003–2012.

Russell, G. L., J. R. Miller, and D. Rind (1995), A coupled atmosphere-ocean model for transient climate change, *Atmos. Ocean*, *33*, 683–730.

Sagan, C., and R. Turco (1990), *A Path Where No Man Thought—Nuclear Winter and the End of the Arms Race*, 499 pp., Random House, New York.

Schmidt, G. A., et al. (2006), Present-day atmospheric simulations using GISS ModelE: Comparison to in situ, satellite, and reanalysis data, *J. Clim.*, *19*, 153–192.

Schneider, S. H., and S. L. Thompson (1988), Simulating the climatic effects of nuclear war, *Nature*, *333*, 221–227.

Stenchikov, G. L., et al. (1998), Radiative forcing from the 1991 Mount Pinatubo volcanic eruption, *J. Geophys. Res.*, *103*, 13,837–13,857.

Stenchikov, G., K. Hamilton, R. J. Stouffer, A. Robock, V. Ramaswamy, B. Santer, and H.-F. Graf (2006a), Climate impacts of volcanic eruptions in the IPCC AR4 climate models, *J. Geophys. Res.*, *111*, D07107, doi:10.1029/2005JD006286.

Stenchikov, G., M. Fromm, and A. Robock (2006b), Regional simulations of stratospheric lofting of smoke plumes, *Eos Trans. AGU*, *87*(52), Fall Meet. Suppl., Abstract U14A-05.

Thompson, S. L. (1985), Global interactive transport simulations of nuclear war smoke, *Nature*, *317*, 35–39.

Thompson, S. L., and S. H. Schneider (1986), Nuclear winter reappraised, *Foreign Affairs*, *64*, 981–1005.

Toon, O. B., R. P. Turco, A. Robock, C. Bardeen, L. Oman, and G. L. Stenchikov (2007), Atmospheric effects and societal consequences of regional scale nuclear conflicts and acts of individual nuclear terrorism, *Atmos. Chem. Phys.*, *7*, 1973–2002.

Turco, R. P., O. B. Toon, T. P. Ackerman, J. B. Pollack, and C. Sagan (1983), Nuclear winter: Global consequences of multiple nuclear explosions, *Science*, *222*, 1283–1292.

Turco, R. P., O. B. Toon, T. P. Ackerman, J. B. Pollack, and C. Sagan (1990), Climate and smoke: An appraisal of nuclear winter, *Science*, *247*, 166–176.

Vogelmann, A. M., A. Robock, and R. G. Ellingson (1988), Effects of dirty snow in nuclear winter simulations, *J. Geophys. Res.*, *93*, 5319–5332.

Vogelmann, A. M., T. P. Ackerman, and R. P. Turco (1992), Enhancements in biologically effective ultraviolet radiation following volcanic eruptions, *Nature*, *359*, 47–49, doi:10.1038/359047a0.

Vonnegut, K. (1969), *Slaughterhouse Five*, 186 pp., Delacorte, New York.

Warren, S. G., and W. J. Wiscombe (1985), Dirty snow after nuclear war, *Nature*, *313*, 467–470.

_____

A. Robock and G. L. Stenchikov, Department of Environmental Sciences, Rutgers University, 14 College Farm Road, New Brunswick, NJ 08901, USA. (robock@envsci.rutgers.edu)

L. Oman, Department of Earth and Planetary Sciences, Johns Hopkins University, Baltimore, MD 21218, USA.